PLANT SCIENCES

Co-condensation with photoexcited cryptochromes facilitates MAC3A to positively control hypocotyl growth in *Arabidopsis*

Bochen Jiang[1]†‡*, Zhenhui Zhong[2]†, Jun Su[3]†, Tengfei Zhu[4], Timothy Yueh[1], Jielena Bragasin[1], Victoria Bu[1], Charles Zhou[1], Chentao Lin[1,3], Xu Wang[4]*

Cryptochromes (CRYs) are blue light receptors that mediate plant photoresponses through regulating gene expressions. We recently reported that *Arabidopsis* CRY2 could form light-elicited liquid condensates to control RNA methylation. However, whether CRY2 condensation is involved in other gene expression–regulatory processes remains unclear. Here, we show that MOS4-associated complex subunits 3A and 3B (MAC3A/3B) are CRY-interacting proteins and assembled into nuclear CRY condensates. *mac3a3b* double mutants exhibit hypersensitive photoinhibition of hypocotyl elongation, suggesting that MAC3A/3B positively control hypocotyl growth. We demonstrate the noncanonical activity of MAC3A as a DNA binding protein that modulates transcription. Genome-wide mapping of MAC3A-binding sites reveals that blue light enhances the association of MAC3A with its DNA targets, which requires CRYs. Further evidence indicates that MAC3A and ELONGATED HYPOCOTYL 5 (HY5) occupy overlapping genomic regions and compete for the same targets. These results argue that photo-condensation of CRYs fine-tunes light-responsive hypocotyl growth by balancing the opposed effects of HY5 and MAC3A.

INTRODUCTION

Cryptochromes (CRYs) are photolyase-like blue light receptors that mediate many aspects of photoresponses in plants (*1*, *2*). CRYs exist as physiologically inactive monomers in the dark, and photon absorption causes conformational change and oligomerization of CRYs, which increases CRYs′ affinities with many other interacting partners to form diverse CRY complexes (*3*, *4*). These CRY complexes affect plant growth and development by regulating the transcription or stability of photoresponsive proteins (*2*). CONSTITUTIVELY PHOTOMORPHOGENIC 1 (COP1) identified as a CRY-signaling protein in plants (*5*, *6*), which interacts with its positive regulator SUPPRESSOR OF phyA-105 1 (SPA1) to function as an E3 ubiquitin ligase (*7*). In *Arabidopsis*, both CRY1 and CRY2 interact with COP1 regardless of light (*5*, *6*), while the light-dependent association of CRY1/CRY2 and SPA1 severely impedes the physiological activities of COP1 (*7*–*11*). Photoactivated CRY1 and CRY2 compete with ELONGATED HYPOCOTYL 5 (HY5) for COP1 binding through conserved Val-Pro motifs (*12*, *13*) and thus stabilize HY5 protein in the light. Accumulated HY5 modulates the expression of more than 3000 genes to promote plant photomorphogenesis (*14*–*17*).

More than 30 CRY-interacting proteins have been identified so far (*2*). Most of these interactions are blue light dependent. Our recent study has found that photo-excited CRY2 undergoes liquid-liquid phase separation (LLPS) to form photobodies, where subunits of the m^{6}A writer complex are co-condensed without changing their apparent affinities with CRY2 (*18*). The elevated local concentration of m^{6}A writer complexes in CRY2 photobodies positively correlates with a global up-regulation of m^{6}A installation on mRNAs (*18*). Accumulated evidence shows that many of the CRY2-interacting partners colocalize with CRY2 photobodies and regulate gene transcriptions during photomorphogenesis. For example, CRY1 and CRY2 interact with HBI1 (HOMO LOG OF BEE2 INTERACTING WITH IBH1) in photobodies and inhibit the transcriptional activity of HBI1 to repress hypocotyl elongation (*19*). The above findings strongly argue that photo-regulated protein condensation may play an important role in light signaling. However, it is still unclear how phase separation affects the molecular activities of proteins.

Here, we report that MOS4-associated complex subunits 3A and 3B (MAC3A/3B), the *Arabidopsis* counterparts of the NINETEEN COMPLEX or Prp19 complex in yeast and humans (*20*), interact with CRYs and are assembled into CRY condensates in a blue light–dependent manner to positively regulate hypocotyl elongation. We demonstrate that MAC3A can function as a DNA binding protein and share thousands of common genomic binding sites with HY5. The in vitro DNA binding assay further reveals that MAC3A competes with HY5 for the same DNA probes. Co-condensation with photoexcited CRYs in blue light may facilitate MAC3A to bind DNA in plants, thus allowing MAC3A to antagonize HY5 activities more intensely. Together, our results argue that CRYs may fine-tune light-responsive hypocotyl growth by balancing the opposed effects of HY5 and MAC3A, and photo-condensation facilitates the refinement of such actions of CRYs.

[1]Department of Molecular, Cell, and Developmental Biology, University of California, Los Angeles, CA 90095, USA. [2]State Key Laboratory for Ecological Pest Control of Fujian and Taiwan Crops, College of Plant Protection, Fujian Agriculture and Forestry University, Fuzhou 350002, China. [3]Basic Forestry and Proteomics Research Center, Fujian Agriculture and Forestry University, Fuzhou 350002, China. [4]Peking University Institute of Advanced Agricultural Sciences, Shandong Laboratory of Advanced Agricultural Sciences at Weifang, Weifang, Shandong 261325, China.
*Corresponding author. Email: bochenj@uchicago.edu (B.J.); xu.wang@pku-iaas.edu.cn (X.W.)
†These authors contributed equally to this work.
‡Present address: Department of Chemistry, The University of Chicago, Chicago, IL 60637, USA.

RESULTS

Blue light promotes MAC3A/3B condensate into the photobodies of CRYs

We previously reported that blue light triggered the co-condensation of the m^{6}A writer complex with CRY2 in liquid CRY2 condensates to maintain the normal circadian rhythms in plants (*18*). We wondered whether other proteins could be assembled into CRY2 condensates to regulate plant photo-responses. Therefore, we profiled the components of CRY2 complexes isolated from transgenic plants overexpressing green fluorescent protein (GFP)–CRY2 using immunoprecipitation (IP) coupled with mass spectrometry (*21*) and identified MOS4-associated complex subunits 3A and 3B as CRY2-associated proteins (fig. S1A). MAC3A/3B are conserved U-box–containing proteins in eukaryotes, which play essential roles in regulating plant immunity and development (*22*–*24*). The co-IP assays in both human embryo kidney (HEK) 293T cells (Fig. 1, A and B) and transgenic *Arabidopsis* plants (Fig. 1C) validated the interactions between CRY1/CRY2 and MAC3A but no light dependency for the interactions was observed.

This prompted us to examine whether MAC3A/3B could co-condense with CRY2 in light-responsive liquid CRY2 condensates. Although MAC3A-GFP fusion protein in transgenic plants uniformly distributed in the nucleoplasm (fig. S1B), we found that MAC3A partially colocalized with CRYs in the nuclear bodies only in the presence of blue light (Fig. 1D), indicating that the location of MAC3A-CRY interactions is light responsive at the subcellular level. Consistent with this evidence, when CRY2/CRY1 and MAC3A/3B were coexpressed as BiFC (bimolecular fluorescence complementation) pairs in blue light–illuminated tobacco leaf epidermal cells, fluorescent speckles of reconstituted yellow fluorescent protein (YFP) were detected (Fig. 1E and fig. S1, C and D), while this punctate pattern of BiFC signals was not observed when MAC3A/3B were paired with the photo-insensitive CRY mutant proteins, CRY1^{D390A} and CRY2^{D387A} (Fig. 1E and fig. S1D) (*2*). These results suggest that MAC3A/3B might be incorporated into CRY condensates in a light-dependent manner, although their interaction affinities are light irresponsive. The mapping of the interacting domain of MAC3A and CRY2 showed that full-length MAC3A was necessary for the interaction with the full-length, N terminus (N489, the photolyase homologous region) and C-terminus (C490, cryptochrome C-terminal extension) of CRY2 (fig. S1D). The fluorescence recovery after photobleaching (FRAP) assay was then used to determine whether CRY-MAC3A co-condensates were in the liquid state. The BiFC signals of either CRY1-MAC3A or CRY2-MAC3A recovered rapidly (within 30 s) after photobleaching (Fig. 1, F and G), while the noncondensed CRY1^{D390A}-MAC3A and CRY2^{D398A}-MAC3A BiFC signals showed a much lower recovery rate after photobleaching (fig. S1E), meaning that CRY-MAC3A molecules in the condensed phase are highly mobile. This result was in line with other evidence that small condensate droplets of CRY-MAC3A tended to coalesce into larger droplets over time in blue light (fig. S1F) and 1,6-hexanediol effectively inhibited the CRY-MAC3A condensates′ formation (fig. S1, G and H). These results strongly agree with the liquid-like properties of CRY-MAC3A condensates. Together, we propose that MAC3A proteins are co-condensed with photoexcited CRYs in the liquid condensates via specific interactions.

MAC3A/3B genetically interact with *CRY1* in blue light to positively regulate hypocotyl elongation

We next investigated the role of *MAC3A/3B* genes in plant photoresponses. Both *mac3a* and *mac3b* single mutants exhibit no discernable phenotypes in hypocotyl growth, but the *mac3amac3b* (referred as *mac3a3b* in the following text) double mutants had much shorter hypocotyls than wild type (WT) in the dark, blue, red, and far-red light (Fig. 2 and fig. S2A), suggesting that *MAC3A/3B* positively control hypocotyl growth under both dark and light conditions. Further analyses on hypocotyl growth response to different blue light fluence rates showed that *mac3a3b* hypocotyls were shorter than WT at all fluence rates tested (Fig. 2, A and B), and the hypocotyl-length ratio between *mac3a3b* and WT showed a decrease in response to increasing fluence rates of blue light (Fig. 2C), suggesting that *mac3a3b* mutants are hypersensitive to the blue light–mediated inhibition of hypocotyl elongation. The short-hypocotyl phenotype of *mac3a3b* mutants in blue light could be rescued by constitutively expressing the MAC3A or MAC3B coding sequence in *mac3a3b* plants (Fig. 2, D and E), confirming that short-hypocotyl was due to the loss of MAC3A/3B activities in plants. It is worth noting that *MAC3A* overexpression lines are indistinguishable from WT in hypocotyl length (fig. S2B), possibly suggesting that other players could be required for *MAC3A/3B*-involved regulation of hypocotyl growth. Our attempt to generate *cry1cry2mac3a3b* quadruple mutants failed by a genetic cross between *mac3a3b* and *cry1cry2*, possibly due to the linkage of *CRY2* (*AT1G04400*) and *MAC3A* (*AT1G04510*). As the distance between the two genomic regions is less than 40 kb, which is approximately 0.16 cM genetic distance in *Arabidopsis* (*25*), a huge segregation population might be needed to obtain *cry1cry2mac3a3b* quadruple mutants. Besides, endogenous *CRY2* only has a minor effect on light-responsive hypocotyl growth compared to *CRY1* (*2*), and we used *cry1mac3a3b* triple mutants to explore the genetic relationship between *MAC3A/3B* and *CRYs* in the control of light-responsive hypocotyl elongation. The hypocotyls of the *cry1mac3a3b* triple mutants were much longer than WT and *mac3a3b* double mutants but slightly shorter than *cry1* single mutants under blue light (Fig. 2, F and G), suggesting that *cry1* is epistatic to *mac3a3b*. The hypocotyl-length ratio (blue light versus dark) for WT and *mac3a3b* mutants was significantly different, while this ratio for *cry1mac3a3b* triple and *cry1* single mutants remained unchanged (Fig. 2H), indicating that the hypersensitive response to the blue light–inhibited hypocotyl elongation in *mac3a3b* mutants is *CRY1* dependent. However, we found that the abundance of neither MAC3A proteins nor mRNA was regulated by light (Fig. 2, I and J) (*26*), implying that other activities of MAC3A might be affected by blue light.

Blue light and CRYs facilitate the association of MAC3A with chromatin in plants

MAC3A/3B have been reported to function as E3 ubiquitin ligases (*22*, *24*); we therefore asked whether MAC3A/3B affect the protein stability of CRYs and thus modulate CRY activities. The immunoblot assay clearly showed that the phosphorylation and degradation of CRYs were not altered in *mac3a3b* seedlings compared to the WT (fig. S3C). Furthermore, the short hypocotyl phenotype of *mac3a3b* mutants was fully complemented by introducing transgenes separately expressing two MAC3A proteins with mutations in the U-box domain, MAC3A^{Mut1} and MAC3A^{Mut2}, both of which lacked

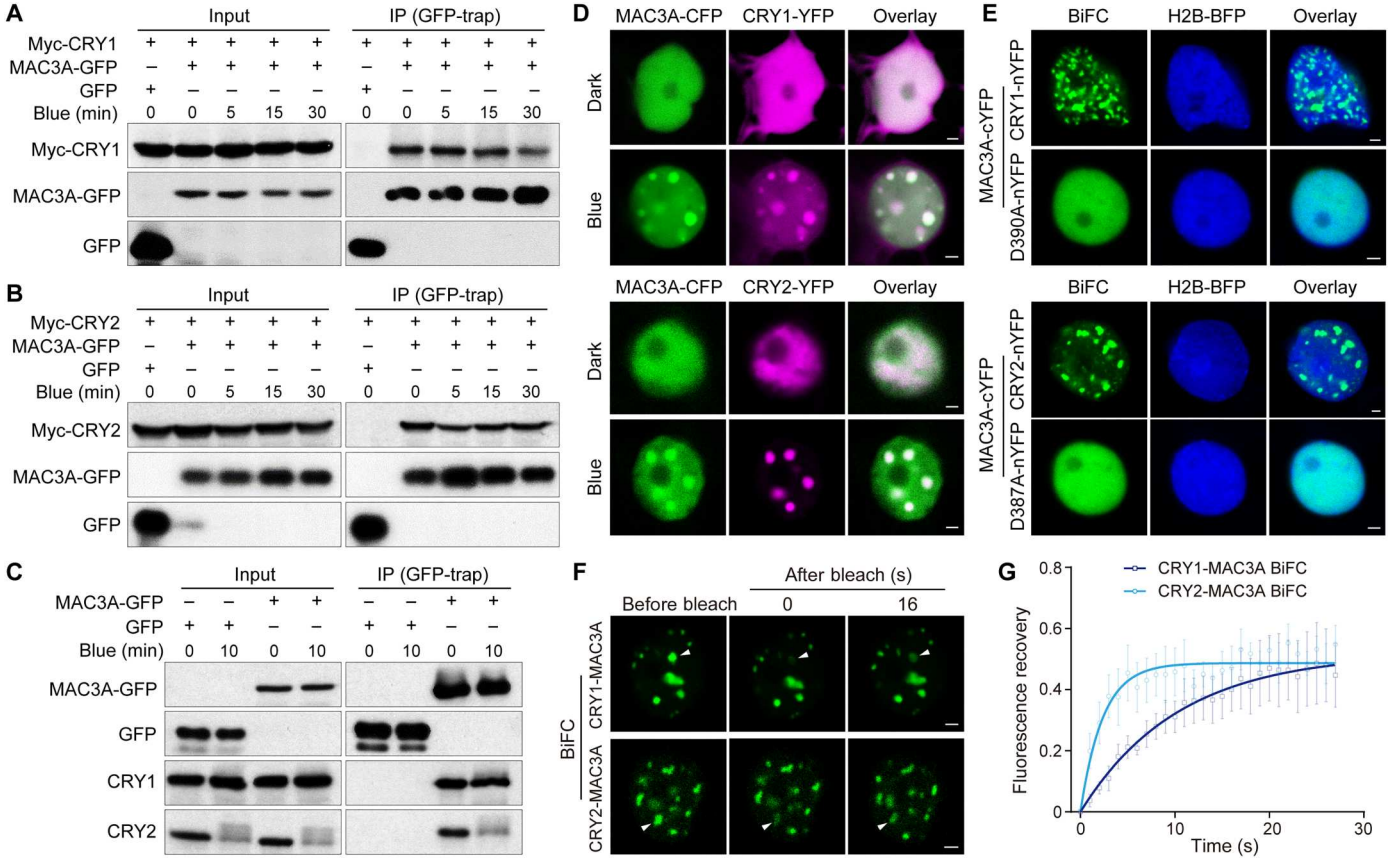

Fig. 1. MAC3A interacts with CRYs and co-condenses with CRYs in nuclear CRY photobodies. (**A** and **B**) Co-IP assays showing the interactions of MAC3A-GFP with Myc-CRY1 (A) or Myc-CRY2 (B) in human HEK293T cells. The cells transfected with plasmids were cultured in the dark and irradiated with blue light (Blue; 100 μmol m^{-2} s^{-1}) for the indicated time before harvest. GFP-trap agarose resin was used for IP. (**C**) Co-IP assay showing the interactions of MAC3A-GFP with endogenous CRY1 and CRY2 in plants. The etiolated seedlings of the *35S::F-MAC3A-GFP* transgenic line were kept in the dark or irradiated with blue light (Blue; 30 μmol m^{-2} s^{-1}) for 10 min before harvesting for the assay. GFP-trap agarose resin was used for IP, and the anti-CRY1 or anti-CRY2 antibodies were used for the immunoblots to detect the endogenous CRY1 or CRY2 proteins, respectively. (**D**) Partial colocalization of MAC3A with CRY1 or CRY2 in nuclear condensates in blue light–illuminated tobacco leaf epidermal cells. Three independent experiments were performed showing similar results. Scale bar, 2 μm. (**E**) BiFC assays showing the interactions of MAC3A/CRY1 or MAC3A/CRY2 in nuclear condensates in blue light–illuminated tobacco leaf epidermal cells. Photo-insensitive $CRY1^{D390A}$ and $CRY2^{D387A}$ were used as the negative control for light-induced CRY condensation. H2B-BFP was used as the nuclear marker. Scale bar, 2 μm. (**F**) FRAP analysis of CRY1/MAC3A or CRY2/MAC3A BiFC signals in the nuclear condensates. The white arrows indicate the region for photo-bleaching. Scale bar, 2 μm. (**G**) Fluorescence recovery of MAC3A/CRY1 or MAC3A/CRY2 BiFC signals in FRAP assay shown in (F). The double exponential fit (solid line) of averaged recovery curves is shown (mean ± SEM, n = 5 independent FRAP experiments).

ubiquitin ligase activities (*24*) (fig. S3, A and B), suggesting that the ubiquitin ligase activity of MAC3A is not necessary for regulating hypocotyl elongation, and other molecular activities of MAC3A must be implicated in this process. As MAC3A is involved in co-transcriptional RNA alternative splicing, we wonder whether MAC3A is able to bind chromatin to regulate transcription. Therefore, we performed chromatin immunoprecipitation followed by sequencing (ChIP-seq) assay using transgenic lines expressing *Flag-MAC3A-GFP* or *Flag-GFP* grown under blue light or dark conditions. This identified tens of thousands of MAC3A-specific genomic binding peaks, suggesting that MAC3A is a chromatin-binding protein. More than 47% of MAC3A-binding peaks are located at the promoter and transcription start site (TSS) and ~12% of the peaks are enriched around the transcription terminal site (TTS) (Fig. 3, A and B). This result uncovers a previously unknown activity of MAC3A that binds chromatin with dual preferences.

Notably, we also found that blue light might facilitate the binding of MAC3A with chromatin based on the following results. First, more MAC3A-binding peaks were identified from the ChIP-seq in blue light–grown samples (n = 11,831 peaks) than in the dark-grown samples (n = 7449 peaks), and the overall intensity of peaks in blue light was significantly higher than that in the dark (P < 0.0001; Fig. 3E), although the enriched motifs under these peaks in both conditions were not varied much (Fig. 3, C and D). Next, MAC3A bound more genes in blue light (n = 10,077) than in the dark (n = 6552) (Fig. 3F). Among those overlapping genes (n = 5388) under both conditions, genes with increased peak intensities in blue light (>2-fold; n = 2243) were ~11 times more than the genes with reduced peak intensities in blue light (<0.5-fold; n = 204) (Fig. 3, G and H), and gene ontology (GO) analysis of those genes whose MAC3A-binding peak intensities were light induced (n = 2243) showed significant enrichment in response to light cues (Fig. 3I). These results strongly argue for the promotion of MAC3A-

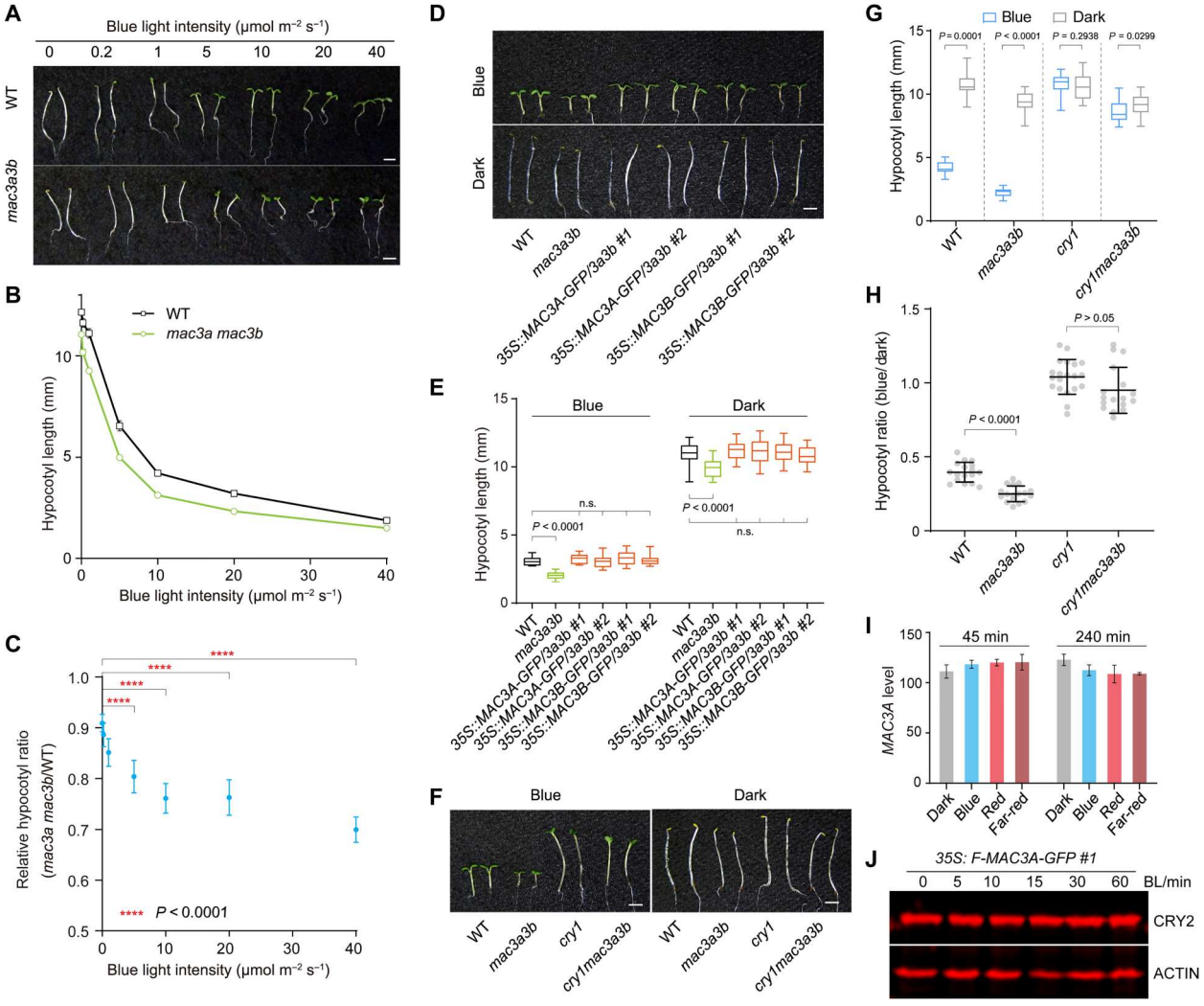

Fig. 2. *MAC3A/3B* genetically interact with *CRY1* in blue light to positively regulate hypocotyl elongation. (**A** and **B**) Measurements of hypocotyl length of indicated genotypes grown in the blue light with different intensities (0, 0.2, 1, 5, 10, 20, and 40 μmol m^{-2} s^{-1}) for 6 days. The hypocotyl phenotypes of different genotypes are shown in (A), and hypocotyl length measurements (B) are shown as mean ± SD. ($n \geq 20$). Scale bar, 2 mm (A). (**C**) Hypocotyl-length ratio of *mac3a3b* versus WT at each fluence rate in the assay shown in (A) and (B). Asterisks indicate significant differences between dark and various blue light intensities ($P < 0.0001$) based on two-tailed Student's *t* test. (**D** to **G**) Measurements of the hypocotyl length of different genotypes grown in the dark or blue light (25 μmol m^{-2} s^{-1}) for 6 days. The hypocotyl phenotypes of indicated genotypes are shown in (D) and (F), and hypocotyl-length measurements are shown as mean ± SD ($n \geq 20$) in (E) and (G). *P* value calculated by two-tailed Student's *t* test is used to determine the statistical significance between genotypes. Scale bars, 2 mm [(D) and (F)]. (**H**) Hypocotyl-length ratio (blue versus dark) for each genotype in the assay shown in (F) and (G). *P* value calculated by two-tailed Student's *t* test was used to determine the statistical significance between genotypes. (**I**) *MAC3A* mRNA levels in WT seedlings treated with different wavelengths for the indicated time (45 and 240 min). The *MAC3A* expression data were obtained from the *Arabidopsis* eFP Browser. (**J**) Immunoblot assay showing the MAC3A protein levels in response to blue light. Seven-day-old etiolated seedlings of the *35S::F-MAC3A-GFP* transgenic line were treated with blue light (25 μmol m^{-2} s^{-1}) for the indicated time and used for protein extraction and immunoblot analysis. Actin was used as the loading control. n.s., not significant.

chromatin association in blue light. We then questioned whether CRY-mediated photo sensing might be responsible for this effect. To this end, we measured the strength of specific MAC3A-chromatin interaction in both WT and *cry1cry2* mutants grown in the dark or blue light by ChIP with quantitative polymerase chain reaction (ChIP-qPCR), and a clear increase of the MAC3A ChIP signal at the *YUC8* promoter in blue light was detected in WT but not in *cry1cry2* (Fig. 3J), indicating that CRYs might mediate the blue light–enhanced binding of MAC3A with chromatin in plants. This might be explained by the light-dependent co-condensation of MAC3A in CRY condensates (Fig. 1, D to G), as following the treatment with the LLPS inhibitor, 1,6-hexanediol, the association of MAC3A with *YUC8* promoter under blue light was notably repressed (fig. S3D). Thus, we propose that this concentrating mechanism of MAC3A by CRY phase separation in blue light might allow direct promotion of MAC3A-chromatin association.

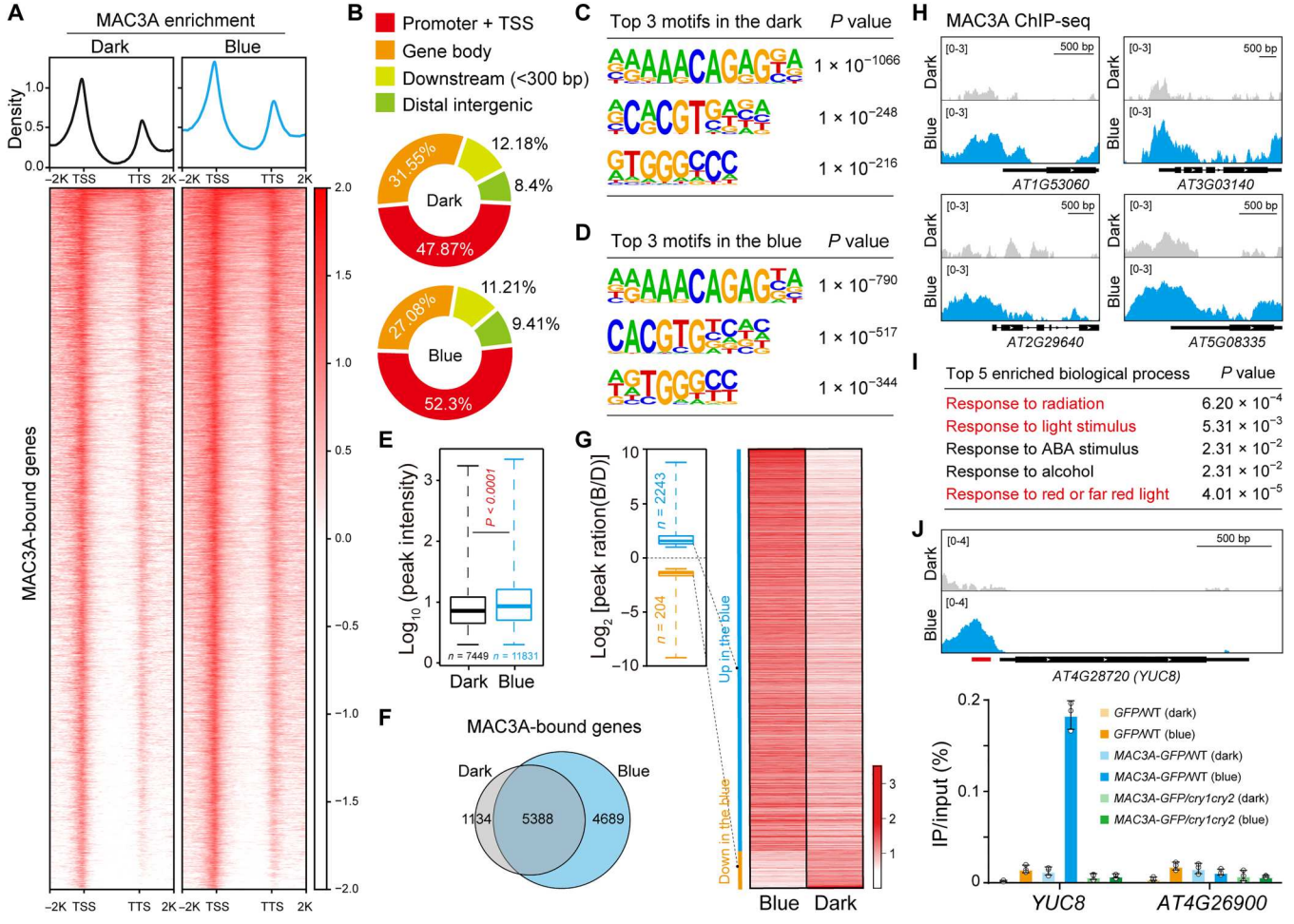

Fig. 3. Blue light and CRYs enhance the association of MAC3A with chromatin. (**A**) Metaplots and heatmaps of MAC3A ChIP-seq reads over genes. The *35S: F-MAC3A-GFP* or *35S: F-GFP* transgenic line grown in the dark (Dark) or blue light (Blue; 25 μmol m^{-2} s^{-1}) were used for ChIP-seq assays. TSS, transcription start site; TTS, transcription terminal site; −2K, 2 kb upstream of TSS; 2K, 2 kb downstream of TTS. (**B**) Pie charts showing the genomic distributions of MAC3A-binding peaks identified in the ChIP-seq assays (A). (**C** and **D**) Top three enriched de novo motifs under the MAC3A-binding peaks, which were located at the promoter and TSS regions. (**E**) Boxplot of the overall peak intensities of MAC3A ChIP-seq in the dark and blue light. *P* value ($P < 0.0001$) calculated by two-tailed Student's *t* test indicated the significant difference between dark and light conditions. (**F**) Venn diagram showing the overlap of MAC3A-bound genes in the dark and blue light. (**G**) Boxplot showing the ratios of peak intensities in blue light over the dark. Only genes with the ratio >2 ($n = 2243$) or <0.5 ($n = 204$) were shown in the plot. The heatmap shows the ChIP-seq peak intensities in the dark or blue light of the selected genes in the boxplot. (**H**) Representative snapshots of MAC3A occupancy over the selected genes showing the blue light–promoted MAC3A-chromatin binding. (**I**) Top five enriched biological processes from GO analysis of the selected genes [$n = 2243$, (G)]. (**J**) Snapshot of MAC3A binding to *YUC8* promoter (top) and the ChIP-qPCR analysis showing the occupancy of MAC3A with *YUC8* promoter region in different genotypes (bottom). The seedlings grown in dark and blue light (25 μmol m^{-2} s^{-1}) were harvested for ChIP-qPCR assay. *At4g26900* locus was used as the negative control. qPCR data are shown as mean ± SD ($n = 3$).

MAC3A and HY5 share overlapping binding regions on the chromatin

We interrogated sequences under MAC3A peaks for enriched motifs and identified the G-box (CACGTG) as one of the top hits (Fig. 3, C and D). This motif primarily associates with the basic region/leucine zipper motif (bZIP) transcription factors, such as *ELONGATED HYPOCOTYL5* (*HY5*), a key regulator of transcriptional networks for photomorphogenesis (*27*, *28*). Using the published HY5 ChIP-seq dataset (fig. S4, C and D) (*17*), we observed a notable overlap of HY5-binding sites and MAC3A-bound promoters (Fig. 4A and fig. S4, A and B). About 62% of the HY5-bound promoters were co-occupied by MAC3A (Fig. 4A); in addition, the binding peaks of both proteins on those promoters were in proximity to each other (fig. S4, A and B). A close examination allowed us to divide the MAC3A-bound promoter peaks in blue light into four groups (Fig. 4, A to D): group 1, MAC3A-specific peaks in both dark and blue light ($n = 3355$); group 2, HY5 and MAC3A co-occupied peaks only in blue light ($n = 648$); group 3, MAC3A-specific peaks only in blue light ($n = 3541$); and group 4, HY5 and MAC3A co-occupied peaks in both dark and blue light ($n = 1028$). Consistent with this high co-occupancy of HY5 and MAC3A on specific chromatin sites, we found that the top five enriched motifs under group 4 promoter peaks were G-box and its variants (Fig. 4E). These results well demonstrate the functional connection of MAC3A and HY5 at the molecular level.

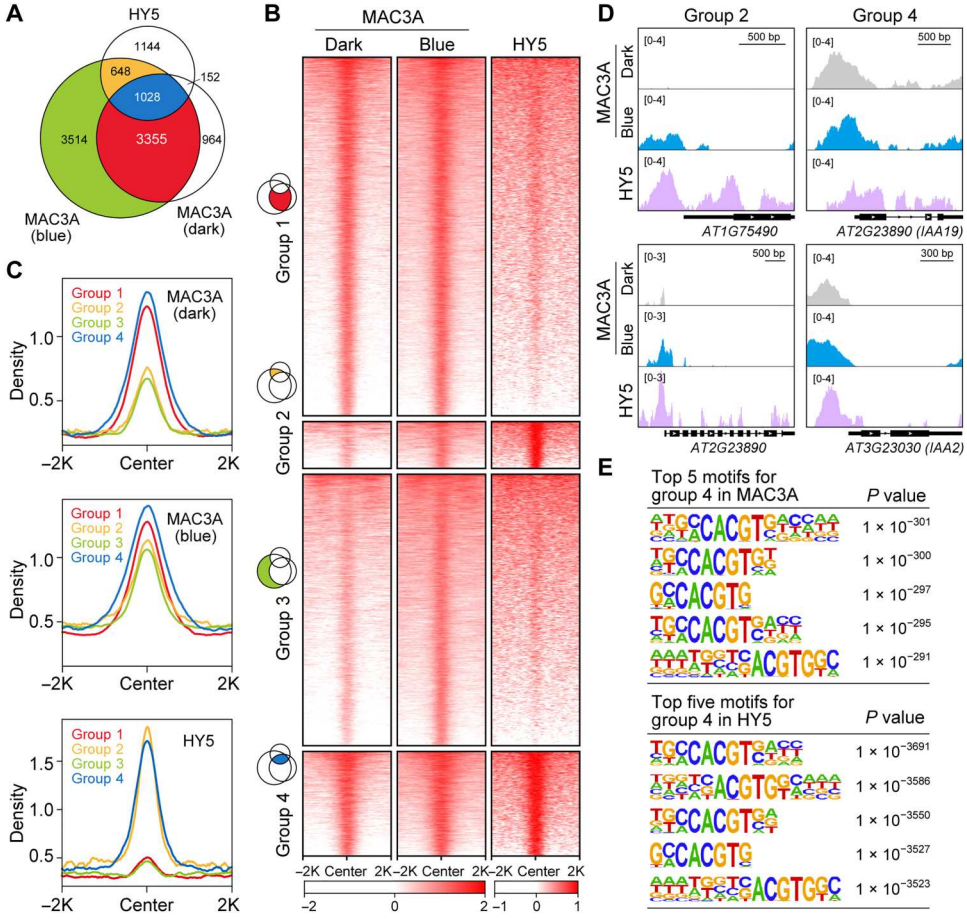

Fig. 4. MAC3A and HY5 share overlapping binding regions on the chromatin. (**A**) Venn diagram showing the overlap of HY5 and MAC3A-bound genes in the dark (MAC3A dark) and blue light (MAC3A blue; 25 μmol m^{-2} s^{-1}). (**B**) Heatmaps of MAC3A-bound genes in blue light, which are divided into four groups. (**C**) Metaplots of MAC3A and HY5 ChIP-seq reads over the genes in the groups shown in (B). (**D**) Representative snapshots of MAC3A and HY5 binding to promoters of the genes in group 2 and group 4 defined in (B). (**E**) Top five enriched motifs under the MAC3A and HY5-binding peaks, which were located at the promoter and TSS regions of the genes in group 4.

Direct competition of MAC3A with HY5 for DNA binding might antagonize HY5 activities in plants

We next tested whether MAC3A could directly bind DNA like HY5 by fluorescence-linked immunosorbent assay (FLISA). Basically, the purified recombinant proteins were incubated with the biotin-labeled DNA probes, which were then captured by neutravidin-coated plates. Protein-specific primary antibodies and fluorescent secondary antibodies were used to quantify the strength of DNA-protein binding (Fig. 5A). Two DNA probes were selected from the promoter regions of *YUC8* and *IAA19*, which were identified as MAC3A and HY5 co-occupied peaks in ChIP-seq assays (Figs. 3J and 4D). In addition, both *YUC8* and *IAA19* have well-established roles in control of hypocotyl elongation (*29*). The biotin-labeled *YUC8* and *IAA19* probes ($pYUC8^{biotin}$ and $pIAA19^{biotin}$) and purified recombinant MAC3A proteins fused to Glutathione-S-transferase (GST) were used for FLISA. The FLISA results showed the direct binding of MAC3A with both DNA probes (Fig. 5B); moreover, the binding signals could be quenched by adding unlabeled DNA probes (i.e., cold probes) to the binding reactions (Fig. 5B). Besides, mutations in the G-box of the two DNA probes ($pYUC8^{Mut}$ and $pIAA19^{Mut}$) notably reduced the binding strength with MAC3A (fig. S5A), suggesting that G-box could be one of the sites bound with MAC3A. The in vitro binding of MAC3A to the DNA probes was orthogonally validated by electrophoretic mobility shift assays (EMSA) as well (Fig. 5C and fig. S5B).

Last, we applied the FLISA to explore whether MAC3A could influence HY5-DNA binding. The results revealed that HY5-DNA binding signals drastically decreased with the increased amount of GST-MAC3A proteins added to the binding reactions, while this influence was not seen when GST proteins were used instead (Fig. 5D). These evidence suggest that MAC3A as a DNA binding protein could compete with HY5 for DNA binding. This finding was also in line with the in vivo ChIP-qPCR results. The ChIP was performed with anti-HY5 antibodies to capture chromatin regions bound with endogenous HY5 in different genotypes grown in blue light. The ChIP-qPCR analyses showed that HY5 bound to *YUC8* and *IAA19* promoters in WT and *mac3a3b* but not in *hy5* mutants (Fig. 5E). Furthermore, the enrichment of HY5 at *YUC8* and *IAA19* promoters was significantly higher in *mac3a3b* mutants than that in WT (Fig. 5E), suggesting that MAC3A might impede the HY5-chromatin association in plants. The competition of MAC3A and HY5 for binding at *YUC8* and *IAA19* promoters led

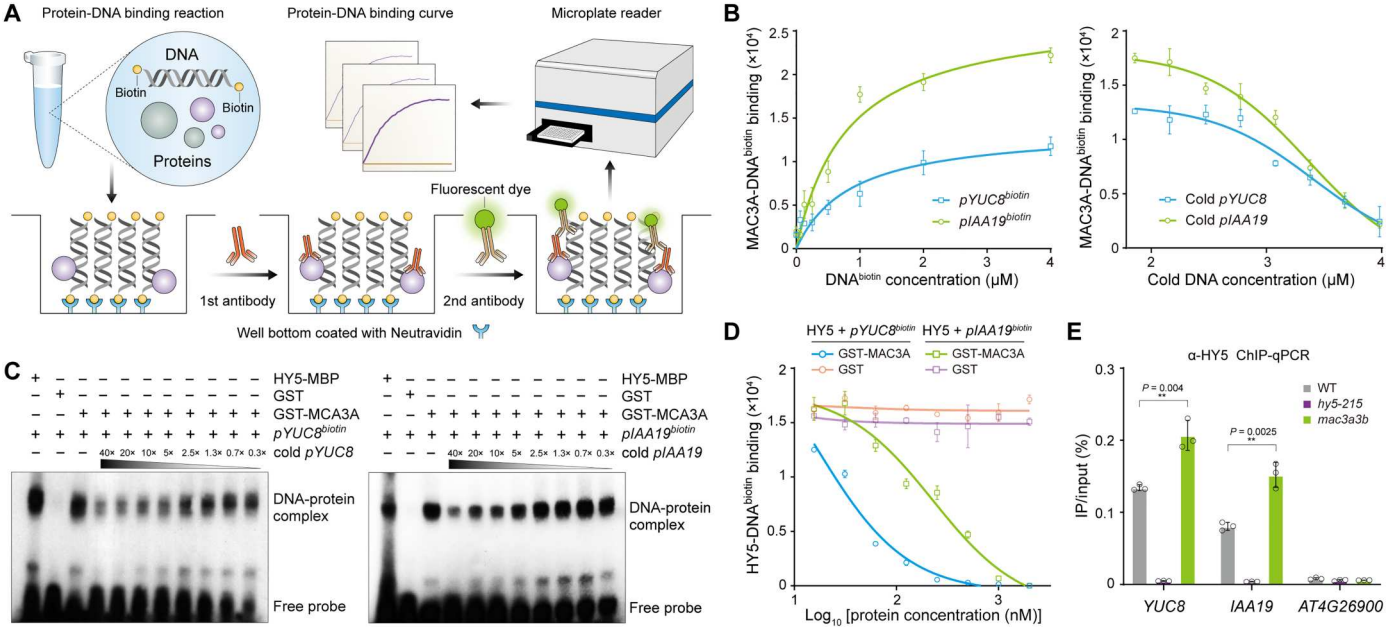

Fig. 5. MAC3A competes with HY5 for DNA binding and attenuates the HY5-chromatin association. (**A**) The diagram of the FLISA used to detect the protein-DNA binding. (**B**) Left: The FLISAs showing the binding kinetics of GST-MAC3A (0.5 μM) to DNA probes with various concentrations. *pYUC8*^{biotin} and *pIAA19*^{biotin} indicate the biotin-labeled *YUC8* and *IAA19* promoter DNA probes. The competition kinetics of unlabeled promoter DNA probes (cold *pYUC8* and *pIAA19*) with biotin-labeled DNA probes (1 μM) in binding to GST-MAC3A proteins (0.5 μM) is shown in the right panel. The data are presented as mean ± SD ($n = 3$). The fitting curves are shown as colored lines. (**C**) EMSAs showing the binding of GST-MAC3A to the promoter DNA probes of *YUC8* and *IAA19*. *pYUC8*^{biotin} and *pIAA19*^{biotin} indicate the biotin-labeled *YUC8* and *IAA19* promoter DNA probes. The unlabeled promoter DNA probes are shown as cold *pYUC8* and *pIAA19*. MBP-HY5-His and GST proteins were used as the positive control and negative control, respectively. (**D**) The FLISA shows the compromised HY5-DNA binding in the presence of GST-MAC3A proteins. The standard DNA-binding reaction composed of biotin-labeled DNA probes (1 μM) and MBP-HY5-His proteins (0.5 μM) were incubated with different amounts of GST-MAC3A proteins. GST proteins were used as a negative control. Each data point was shown as mean ± SD ($n = 3$). The fitting curves are shown as colored lines. (**E**) ChIP-qPCR analysis showing the association of the endogenous HY5 proteins with *YUC8* and *IAA19* promoters in genotypes. The seedlings grown in blue light (25 μmol m^{-2} s^{-1}) for 6 days were harvested for ChIP-qPCR analysis using anti-HY5 antibodies. *At4g26900* locus was used as the negative control. The data are shown as mean ± SD ($n = 3$). Asterisks indicate significant difference between WT and *mac3a3b* mutants ($P < 0.01$) based on two-tailed Student's *t* test.

to the alteration of light-responsive expressions of both genes. qPCR analysis revealed that light-suppressed *YUC8* and *IAA19* mRNA expressions were significantly up-regulated in *hy5* mutants and down-regulated in *mac3a3b* mutants compared with the WT (Fig. 6C and fig. S6, A and B); this gene expression pattern is well consistent with the hypocotyl phenotypes for both mutants. The contrary influences of MAC3A and HY5 on regulating gene expression were also seen on other MAC3A and HY5 cotarget genes, such as *SAUR10* and *CHS* (fig. S6, C to H). The functional relevance of *MAC3A* and *HY5* was also supported by genetic evidence. In contrast to the light-hypersensitive short-hypocotyl phenotype of *mac3a3b*, the *hy5mac3a3b* triple mutants showed light-hyposensitive long hypocotyls in blue light (Fig. 6, A and B). Besides, anthocyanin content in *mac3a3b* was significantly higher in blue light than WT and *hy5-215* mutants displayed low anthocyanin phenotype, while additional mutation of *HY5* strongly repressed the high anthocyanin phenotype of *mac3a3b* mutants (fig. S6I). These results suggest that *MAC3A/3B* might act antagonistically toward *HY5* in plants. Together, our results indicate that MAC3A might compete with HY5 for DNA binding, thereby attenuating the HY5-chromatin association to modulate gene expressions and positively regulate hypocotyl elongation in blue light (Fig. 6D).

DISCUSSION

We previously reported that CRY2 and the m^6A writer complex are co-condensed in the liquid CRY2 photobodies to mediate the light-dependent regulation of mRNA methylation and circadian clock entrainment (*18*). In this study, we uncover the function of CRY condensation in regulating gene transcription. Two DNA binding proteins, MAC3A/3B, have been identified and characterized to co-condense with photoexcited CRYs to directly compete with HY5 for DNA binding and positively modulate hypocotyl elongation in blue light.

Arabidopsis MAC3A and MAC3B are the core subunits of the MAC complex. Many of the components in the MAC complex are involved in alternative splicing of mRNA (*22*, *30*). Through their E3 ubiquitin ligase activity, MAC3A/3B also regulate microRNA (miRNA) levels by influencing pri-miRNA transcription, processing, and stability (*23*, *24*). In addition, it has been shown that MAC3A/3B interact with PLEIOTROPIC REGULATORY LOCUS 1 (PRL1) and SNW/SKI-INTERACTING PROTEIN (SKIP) to modulate the splicing of pre-mRNAs transcribed by circadian clock and abiotic stress response–related genes (*24*, *31*, *32*). More recently, histone deacetylases 15 (HDA15) has been reported to regulate abscisic acid (ABA) responses by interacting with MAC3A/3B, which control the intron splicing (*33*). The global splicing defect caused by the loss of function of MAC3A/3B is detected not only

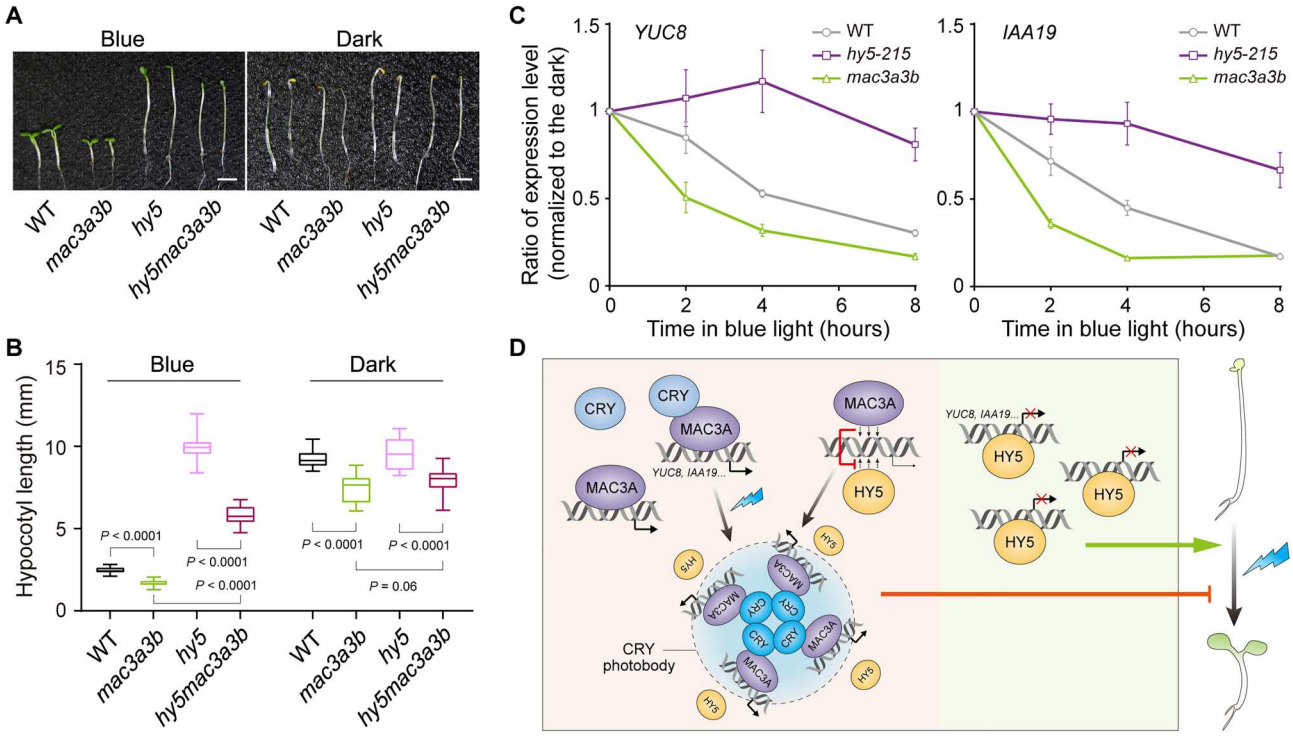

Fig. 6. MAC3A/3B positively control hypocotyl growth partly through antagonizing HY5 activity. (**A** and **B**) Hypocotyl length measurements of the seedlings grown in the dark or blue light (25 μmol m^{-2} s^{-1}) for 6 days. The hypocotyl phenotypes of indicated genotypes are shown in (A), and hypocotyl-length measurements (B) are presented as mean ± SD ($n \geq 20$). *P* value calculated by two-tailed Student's *t* test was used to determine the statistical significance between genotypes. Scale bar, 5 mm (A). (**C**) qPCR analysis showing the light-responsive expressions of *YUC8* and *IAA19* in different genotypes. The etiolated seedlings of indicated genotypes were kept in the dark or treated with blue light (25 μmol m^{-2} s^{-1}) for the indicated time and were used for gene expression analysis. The expression level for each gene at each time point was normalized to the expression level in the dark (i.e., 0 hours in blue light) to obtain the ratio for each time point. The data are presented as means ± SD ($n = 3$). (**D**) A hypothetical model depicting the mechanism of CRYs-mediated photo-regulation of MAC3A on antagonizing HY5 and positively controlling hypocotyl growth. In blue light, accumulated HY5 proteins repress hypocotyl elongation by regulating gene expressions. Meanwhile, CRYs undergo LLPS to condense MAC3A into photobodies; this concentrating mechanism facilitates MAC3A to compete with HY5 for DNA binding, thus attenuating the HY5 transcription-regulatory activity and positively controlling hypocotyl growth.

in mature RNAs but also in nascent RNAs, suggesting a widespread role of MAC3A/3B in co-transcriptional splicing (*34*). However, the lack of significant correlation between intron retention and gene misexpression in *mac3a3b* mutants argues that MAC3A/3B may have separated functions in regulating gene expression and RNA splicing (*23*). In this study, we show that the E3 ubiquitin ligase activity of MAC3A/3B is not essential for controlling hypocotyl growth (fig. S3, A and B), instead the DNA binding activity of MAC3A reported here might play important roles in control of hypocotyl growth (Figs. 3 to 6). However, it is still not clear which domain of MAC3A mediates the DNA binding and whether the DNA binding activity of MAC3A is sufficient for regulating hypocotyl elongation. More biochemical and genetic evidence might help to answer these questions. MAC3A ChIP-seq results revealed that MAC3A were preferentially enriched near TSSs and TTSs (Fig. 3, A and B), which is not common for typical transcription factors, such as HY5. For example, more than 52% of HY5-bound peaks were located near promoter and TSS, whereas only 1.1% were identified around TTS (fig. S4, C and D). Therefore, it is conceivable that promoter and TSS-bound MAC3A are required for modulating gene transcription. Whether and how TTS-bound MAC3A is involved in the regulation of gene expression remains elusive. In addition, both TSS and the 200–base pair (bp) downstream regions are associated with histone H4 lysine 16 acetylation (H4K16ac) marks (*35*), and it would be interesting to investigate whether MAC3A could affect the H4K16ac level to regulate gene expressions.

To fine-tune the *HY5* activity during photomorphogenesis in blue light, plants have developed elaborate yet delicate regulatory mechanisms. CRY1 and CRY2 interact with SPA proteins in a blue light–dependent manner to suppress COP1/SPA activity, partially resulting in the blue light–dependent stabilization of HY5 proteins (*2*, *10*, *11*). In addition, CRY1 promotes H2A.Z deposition to regulate HY5 target gene expression in blue light via the enhancement of both SWR1 complex activity and HY5 recruitment of the SWR1 complex to HY5 target loci (*36*). Blue light–activated CRY1 competes with G-protein β subunit (AGB1) for the binding of HY5, to restore the DNA binding activity of HY5 (*37*). Furthermore, COLD REGULATED GENE 27 and 28 (COR27/28) physically interact with HY5 and associate with the promoters of HY5 target genes, to regulate their transcription (*16*). Here, we demonstrate that MAC3A works as a DNA binding protein and co-condenses with photoexcited CRYs in CRY photobodies, which might facilitate MAC3A to compete with HY5 for binding to promoters of target genes. Thus, CRY-adjusted balancing of the positive effects of HY5 and the negative effects of MAC3A might help to optimize the photomorphogenic growth of plants. Besides, *mac3a3b* mutants

also exhibit short-hypocotyl phenotypes in the dark, red, and far-red light (fig. S2A), and it is tempting to investigate whether MAC3A/3B mediate the co-action of phytochromes and CRYs under natural light conditions and the additional role of MAC3A/3B in the darkness.

MATERIALS AND METHODS

Plant materials and growth conditions

All WT, mutants, and transgenic lines used in this study were *Arabidopsis thaliana* Columbia (Col) accessions. *cry1-304*, *cry1cry2*, *mac3a3b* (*mac3a* allele is SALK_089300; *mac3b* allele is SALK_050811), *pro35S::MAC3A^{Mut1}-GFP* transgenic line, *pro35S::MAC3A^{Mut2}-GFP* transgenic line, and *hy5-215* are described previously (*22*–*24*, *38*, *39*). To prepare transgenic lines overexpressing *35S::F-MAC3A-GFP* or *35S::F-MAC3B-GFP*, constructs were introduced into Col-4 and *mac3a3b* mutants through Agrobacterium-mediated floral dipping (*40*). Light-emitting diode was used to obtain monochromatic blue light, and cool white fluorescent tubes were used as the source for the white light. To prepare *35S::F-MAC3A-GFP* or *35S::F-MAC3B-GFP* binary plasmid, the coding sequence of *MAC3A* or *MAC3B*, which were PCR amplified from *Arabidopsis* complementary DNA (cDNA), was cloned into Xma I–digested *35S::Flag-GFP* vector through in-fusion reaction. The primers used are listed in table S1.

All seeds were sterilized in 10% sodium hypochlorite solution and washed five times with deionized water and then grown on Murashige and Skoog medium (Sigma-Aldrich) supplemented with 0.8% agar and 1.5% sucrose. Seedlings used for the experiments in this study were grown either in the growth chamber (model no. E7/2, Conviron) or in a greenhouse at 22°C with different light regimes.

Protein expression and co-IP assays in HEK293T cells

Assays were performed as described previously (*21*). HEK293T cells were routinely cultured in Dulbecco′s modified Eagle′s medium supplemented with 10% (v/v) fetal bovine serum, 100 IU penicillin, and streptomycin (100 mg/liter) in humidified 5% (v/v) CO_2 in the air, at 37°C. The coding sequences of *Arabidopsis* CRY1, CRY2, and MAC3A were subcloned into modified pEGFP-N1 vectors (Clontech) resulting in genes fused with the DNA sequence encoding the Myc or Flag-GFP epitope tags. The primers used are listed in table S1. Cells transfected with different plasmid DNA were lysed in 800 μl of 1% Brij buffer [1% Brij-35, 50 mM tris-HCl (pH 8.0), 150 mM NaCl, 1 mM EDTA, and 1× protease inhibitor cocktail] rotating at 4°C for 20 min. Cell lysates were centrifuged at 16,000 relative centrifugal force (RCF) for 10 min at 4°C, and the supernatants were incubated with 20 μl of anti-FLAG M2 affinity gel (Sigma-Aldrich) at 4°C for 2 hours with rotation. Beads were washed with 1% Brij buffer five times. Proteins were competed from the beads with 35 μl of 3× Flag peptide solution (200 ng/μl in 1% Brij buffer) for 30 min at room temperature with mixing. Elution was transferred to a new tube, mixed with 4× SDS sample buffer, denatured at 100°C for 5 min, and subjected to Western blot analysis. Primary antibodies used here were anti-Flag (1:1500; Sigma-Aldrich), and anti-Myc (1:5000; Millipore) secondary antibodies used were anti-mouse horseradish peroxidase (HRP) (1:10,000; Thermo Fisher Scientific) and anti-rabbit HRP (1:10,000; catalog no. 31460, Thermo Fisher Scientific).

co-IP assays in *Arabidopsis* plants

The *35S::F-MAC3A-GFP* transgenic plants were grown in the growth chamber for 6 days. The total proteins were extracted with extraction buffer containing 150 mM NaCl, 10 mM tris-HCl (pH 7.5), 2 mM EDTA, 0.5% NP-40, and 1× protease inhibitor cocktail (Roche). Then, the protein extracts were incubated with GFP-trap resin at 4°C for 2 hours. Samples were washed five times with the extraction buffer and competed from the beads with 35 μl of 3× Flag peptide solution and then used for immunoblotting with anti-Flag, anti-CRY1, and anti-CRY2 antibodies (*41*), respectively.

Confocal image acquisition and analysis

The microscopic pictures were acquired using the Zeiss LSM 780 confocal microscope equipped with a Plan-Apochromat 40×/1.40 oil differential interference contrast (DIC) M27 objective. To observe CRY1 or CRY2 photobodies, the slide was put under a microscope, and a 488-nm laser (2% of the laser power) was used to illuminate the samples for the blue light treatment. The images were captured with the 488-nm laser turned off (as dark), and the remaining images were captured with the 488-nm laser on (2% of laser power) as blue light. FRAP tests of photobodies were conducted as previously reported (*2*).

BiFC assay

BiFC assays in tobacco were performed as previously described (*2*) with modifications. The coding sequences of *Arabidopsis* CRY1, CRY2, CRY2-N489 (indicates 1 to 489 amino acids of CRY2 protein), CRY2-C490 (indicates the 490 to 612 amino acids of CRY2 protein), MAC3A, MAC3A-N130 (indicates 1 to 131 amino acids of MAC3A protein), and MAC3A-C131 (indicates 131 to 523 amino acids of MAC3A protein) were amplified for in-fusion into restriction enzyme Xma I–digested *35S::nYFP* or *35S::cYFP* vectors. The resulting vectors were introduced into *Agrobacterium* strain AGL0, which were used for tobacco infiltration (*18*). Tobacco leaves transformed with BiFC plasmids were incubated in the dark for 24 hours before confocal microscopy. At least three independent BiFC experiments were performed for each combination of vectors tested.

Immunoblot assay

Total proteins of *Arabidopsis* seedlings were extracted using protein extraction buffer [120 mM tris (pH 6.8), 100 mM EDTA, 4% (w/v) SDS, 10% (v/v) β-mercaptoethanol, 5% (v/v) glycerol, and 0.05% (w/v) bromophenol]. The total proteins were then separated on 10% SDS–polyacrylamide gel electrophoresis gels and subsequently transferred to nitrocellulose membranes (Pall Life Sciences). Immunoblotting was performed using anti-Flag antibodies (Sigma-Aldrich).

RNA extraction and qPCR assays

The seedlings grown in the dark and then treated with blue light were harvested for total RNA extraction. cDNA was synthesized from 1 μg of total RNA with oligo(dT) primers using the SuperScript IV First-Strand Synthesis System (catalog no. 18091050, Invitrogen). qPCR was performed with gene-specific primers and SYBR Green qPCR SuperMix-UDG (catalog no. 11733-038, Invitrogen) on the Mx3005P Real-Time PCR System (Stratagene). The primer sequences are listed in table S1.

Fluorescence-linked immunosorbent assay

The proteins (1 μM) were incubated with biotin-labeled DNA probes (with different concentrations) in the reaction buffer containing 20 mM tris-HCl (pH 7.4) at 25°C for 30 min, and then the reaction mixtures were transferred to neutravidin-coated 96-well plates and incubated for 30 min at 22°C. The plate was incubated with anti-GST or anti-His antibodies as primary antibodies, and then the fluorescence-conjugated secondary antibody (Thermo Fisher Scientific) was used for detection. The fluorescence signal was measured as the binding activity. Reactions without the DNA probe were used to measure the background signals.

Electrophoretic mobility shift assays

EMSA was performed using the LightShift Chemiluminescent EMSA Kit (Thermo Fisher Scientific) with minor modifications. Briefly, 1 μM purified protein was added to the binding reaction. The binding reactions were kept at 25°C for 25 min in a thermal cycler (Bio-Rad). The sequences of the complementary oligonucleotides used to generate the biotin-labeled and unlabeled DNA probes are shown in table S1.

ChIP assays

Transgenic lines expressing MAC3A-GFP or GFP were used in parallel for ChIP-seq assays. About 2 to 4 g of plant materials was collected and ground with liquid nitrogen. Nuclei isolation buffering (50 mM Hepes, 1 M sucrose, 5 mM KCl, 5 mM $MgCl_2$, 0.6% Triton X-100, 0.4 mM phenylmethylsulfonyl fluoride, and 5 mM benzamidine) containing 1% formaldehyde was used to fix the chromatin for 10 min. Freshly prepared glycine was used to terminate the cross-reaction and sheared via Bioruptor Plus (Diagenode) and immunoprecipitated with the antibody at 4°C overnight. Magnetic Protein A and Protein G Dynabeads (Invitrogen) were added into the samples and incubated at 4°C for 2 hours. The reverse cross-link was performed at 65°C overnight. The protein-DNA mix was treated with protease K (Invitrogen) at 45°C for 4 hours, and then the DNA was purified and precipitated with 3 M sodium acetate (Invitrogen), GlycoBlue (Invitrogen), and ethanol at −20°C overnight. The precipitated DNA was used for qPCR using the primers listed in table S1 or library preparation with an Ovation Ultra Low System V2 kit (NuGEN) following the manufacturer's instructions and sequenced on Illumina NovaSeq.

ChIP-seq data analysis

ChIP-seq reads from this study and published previously (*17*) were mapped to the TAIR10 reference genome with Bowtie2 (v2.1.0) and allowed reads with one best hit and no mismatches (*42*). Duplicated reads were removed by SAMtools. ChIP-seq peaks were called by model-based analysis of ChIP-Seq (MACS2) (v2.1.1) and annotated using ChIPseeker (*43*). Genes with binding peaks at −1000 to +100 bp of the TSS were defined as bound genes. The metaplots were plotted by deeptools (v2.5.1) (*44*). Differentially bound peaks between MAC3A and HY5 were identified by comparing peak files with the merge Peaks function in Homer2, and peaks with a distance of more than 500 bp were defined as differential peaks. Motif enrichment analysis was performed with peak summit extend up and down sequences of 50 bp.

Measurement of anthocyanin contents

The anthocyanin content was determined as described with minor modifications (*45*). Twenty to 30 seedlings were soaked in the extraction buffer (methanol:water:concentrated HCl = 80:20:1) with gentle shaking in the dark. At the end of 24 hours, the extract was read at 530 and 657 nm. Anthocyanin concentration was determined by the formula [A] = A530 − 1/3 × A657 and was given as A/g fresh weight of leaf tissue.

Supplementary Materials

This PDF file includes:
Figs. S1 to S6
Legends for tables S1 to S4

Other Supplementary Material for this manuscript includes the following:
Tables S1 to S4

REFERENCES AND NOTES

1. A. R. Cashmore, Cryptochromes: Enabling plants and animals to determine circadian time. *Cell* **114**, 537–543 (2003).
2. Q. Wang, C. Lin, Mechanisms of cryptochrome-mediated photoresponses in plants. *Annu. Rev. Plant Biol.* **71**, 103–129 (2020).
3. Q. Wang, Z. Zuo, X. Wang, L. Gu, T. Yoshizumi, Z. Yang, L. Yang, Q. Liu, W. Liu, Y. J. Han, J. I. Kim, B. Liu, J. A. Wohlschlegel, M. Matsui, Y. Oka, C. Lin, Photoactivation and inactivation of *Arabidopsis* cryptochrome 2. *Science* **354**, 343–347 (2016).
4. Q. Liu, T. Su, W. He, H. Ren, S. Liu, Y. Chen, L. Gao, X. Hu, H. Lu, S. Cao, Y. Huang, X. Wang, Q. Wang, C. Lin, Photooligomerization determines photosensitivity and photoreactivity of plant cryptochromes. *Mol. Plant* **13**, 398–413 (2020).
5. H. Wang, L. G. Ma, J. M. Li, H. Y. Zhao, X. W. Deng, Direct interaction of *Arabidopsis* cryptochromes with COP1 in light control development. *Science* **294**, 154–158 (2001).
6. H. Q. Yang, R. H. Tang, A. R. Cashmore, The signaling mechanism of *Arabidopsis* CRY1 involves direct interaction with COP1. *Plant Cell* **13**, 2573–2587 (2001).
7. Y. Saijo, J. A. Sullivan, H. Wang, J. Yang, Y. Shen, V. Rubio, L. Ma, U. Hoecker, X. W. Deng, The COP1-SPA1 interaction defines a critical step in phytochrome A-mediated regulation of HY5 activity. *Genes Dev.* **17**, 2642–2647 (2003).
8. H. S. Seo, J. Y. Yang, M. Ishikawa, C. Bolle, M. L. Ballesteros, N. H. Chua, LAF1 ubiquitination by COP1 controls photomorphogenesis and is stimulated by SPA1. *Nature* **423**, 995–999 (2003).
9. D. Zhu, A. Maier, J. H. Lee, S. Laubinger, Y. Saijo, H. Wang, L. J. Qu, U. Hoecker, X. W. Deng, Biochemical characterization of *Arabidopsis* complexes containing constitutively photomorphogenic1 and suppressor of PHYA proteins in light control of plant development. *Plant Cell* **20**, 2307–2323 (2008).
10. B. Liu, Z. Zuo, H. Liu, X. Liu, C. Lin, *Arabidopsis* cryptochrome 1 interacts with SPA1 to suppress COP1 activity in response to blue light. *Genes Dev.* **25**, 1029–1034 (2011).
11. Z. Zuo, H. Liu, B. Liu, X. Liu, C. Lin, Blue light-dependent interaction of CRY2 with SPA1 regulates COP1 activity and floral initiation in *Arabidopsis*. *Curr. Biol.* **21**, 841–847 (2011).
12. K. Lau, R. Podolec, R. Chappuis, R. Ulm, M. Hothorn, Plant photoreceptors and their signaling components compete for COP1 binding via VP peptide motifs. *EMBO J.* **38**, e102140 (2019).
13. J. Ponnu, T. Riedel, E. Penner, A. Schrader, U. Hoecker, Cryptochrome 2 competes with COP1 substrates to repress COP1 ubiquitin ligase activity during *Arabidopsis* photomorphogenesis. *Proc. Natl. Acad. Sci. U.S.A.* **116**, 27133–27141 (2019).
14. J. Lee, K. He, V. Stolc, H. Lee, P. Figueroa, Y. Gao, W. Tongprasit, H. Zhao, I. Lee, X. W. Deng, Analysis of transcription factor HY5 genomic binding sites revealed its hierarchical role in light regulation of development. *Plant Cell* **19**, 731–749 (2007).
15. Y. Burko, A. Seluzicki, M. Zander, U. V. Pedmale, J. R. Ecker, J. Chory, Chimeric activators and repressors define HY5 activity and reveal a light-regulated feedback mechanism. *Plant Cell* **32**, 967–983 (2020).
16. X. Li, C. Liu, Z. Zhao, D. Ma, J. Zhang, Y. Yang, Y. Liu, H. Liu, COR27 and COR28 are novel regulators of the COP1-HY5 regulatory hub and photomorphogenesis in *Arabidopsis*. *Plant Cell* **32**, 3139–3154 (2020).
17. E. Canibano, C. Bourbousse, M. Garcia-Leon, B. Garnelo Gomez, L. Wolff, C. Garcia-Baudino, R. Lozano-Duran, F. Barneche, V. Rubio, S. Fonseca, DET1-mediated COP1 regulation avoids

HY5 activity over second-site gene targets to tune plant photomorphogenesis. *Mol. Plant* **14**, 963–982 (2021).
18. X. Wang, B. Jiang, L. Gu, Y. Chen, M. Mora, M. Zhu, E. Noory, Q. Wang, C. Lin, A photoregulatory mechanism of the circadian clock in *Arabidopsis*. *Nat. Plants* **7**, 1397–1408 (2021).
19. S. Wang, L. Li, P. Xu, H. Lian, W. Wang, F. Xu, Z. Mao, T. Zhang, H. Yang, CRY1 interacts directly with HBI1 to regulate its transcriptional activity and photomorphogenesis in *Arabidopsis*. *J. Exp. Bot.* **69**, 3867–3881 (2018).
20. K. Palma, Q. Zhao, Y. T. Cheng, D. Bi, J. Monaghan, W. Cheng, Y. Zhang, X. Li, Regulation of plant innate immunity by three proteins in a complex conserved across the plant and animal kingdoms. *Genes Dev.* **21**, 1484–1493 (2007).
21. Y. Chen, X. Hu, S. Liu, T. Su, H. Huang, H. Ren, Z. Gao, X. Wang, D. Lin, J. A. Wohlschlegel, Q. Wang, C. Lin, Regulation of *Arabidopsis* photoreceptor CRY2 by two distinct E3 ubiquitin ligases. *Nat. Commun.* **12**, 2155 (2021).
22. J. Monaghan, F. Xu, M. Gao, Q. Zhao, K. Palma, C. Long, S. Chen, Y. Zhang, X. Li, Two Prp19-like U-box proteins in the MOS4-associated complex play redundant roles in plant innate immunity. *PLOS Pathog.* **5**, e1000526 (2009).
23. T. Jia, B. Zhang, C. You, Y. Zhang, L. Zeng, S. Li, K. C. M. Johnson, B. Yu, X. Li, X. Chen, The *Arabidopsis* MOS4-associated complex promotes microRNA biogenesis and precursor messenger RNA splicing. *Plant Cell* **29**, 2626–2643 (2017).
24. S. Li, K. Liu, B. Zhou, M. Li, S. Zhang, L. Zeng, C. Zhang, B. Yu, MAC3A and MAC3B, two core subunits of the MOS4-associated complex, positively influence miRNA biogenesis. *Plant Cell* **30**, 481–494 (2018).
25. W. Lukowitz, C. Gillmor, W. Scheible, Positional cloning in *Arabidopsis*. Why it feels good to have a genome initiative working for you. *Plant Physiol.* **123**, 795–806 (2000).
26. D. Winter, B. Vinegar, H. Nahal, R. Ammar, G. V. Wilson, N. J. Provart, An "electronic fluorescent pictograph" browser for exploring and analyzing large-scale biological data sets. *PLOS ONE* **2**, e718 (2007).
27. N. Abbas, J. P. Maurya, D. Senapati, S. N. Gangappa, S. Chattopadhyay, *Arabidopsis* CAM7 and HY5 physically interact and directly bind to the HY5 promoter to regulate its expression and thereby promote photomorphogenesis. *Plant Cell* **26**, 1036–1052 (2014).
28. M. Binkert, L. Kozma-Bognar, K. Terecskei, L. De Veylder, F. Nagy, R. Ulm, UV-B-responsive association of the *Arabidopsis* bZIP transcription factor elongated hypocotyl5 with target genes, including its own promoter. *Plant Cell* **26**, 4200–4213 (2014).
29. J. Huai, X. Zhang, J. Li, T. Ma, P. Zha, Y. Jing, R. Lin, SEUSS and PIF4 coordinately regulate light and temperature signaling pathways to control plant growth. *Mol. Plant* **13**, 1825 (2020).
30. S. Zhang, Y. Liu, B. Yu, PRL1, an RNA-binding protein, positively regulates the accumulation of miRNAs and siRNAs in *Arabidopsis*. *PLOS Genet.* **10**, e1004841 (2014).
31. A. Feke, W. Liu, J. Hong, M. W. Li, C. M. Lee, E. K. Zhou, J. M. Gendron, Decoys provide a scalable platform for the identification of plant E3 ubiquitin ligases that regulate circadian function. *eLife* **8**, e44558 (2019).
32. Y. Li, J. Yang, X. Shang, W. Lv, C. Xia, C. Wang, J. Feng, Y. Cao, H. He, L. Li, L. Ma, SKIP regulates environmental fitness and floral transition by forming two distinct complexes in *Arabidopsis*. *New Phytol.* **224**, 321–335 (2019).
33. Y.-T. Tu, C.-Y. Chen, Y.-S. Huang, C.-H. Chang, M.-R. Yen, J.-W. A. Hsieh, P.-Y. Chen, K. Wu, HISTONE DEACETYLASE 15 and MOS4-associated complex subunits 3A/3B coregulate intron retention of ABA-responsive genes. *Plant Physiol.* **190**, 882–897 (2022).
34. S. Li, Y. Wang, Y. Zhao, X. Zhao, X. Chen, Z. Gong, Global co-transcriptional splicing in *Arabidopsis* and the correlation with splicing regulation in mature RNAs. *Mol. Plant* **13**, 266–277 (2020).
35. L. Lu, X. Chen, D. Sanders, S. Qian, X. Zhong, High-resolution mapping of H4K16 and H3K23 acetylation reveals conserved and unique distribution patterns in *Arabidopsis* and rice. *Epigenetics* **10**, 1044–1053 (2015).
36. Z. Mao, X. Wei, L. Li, P. Xu, J. Zhang, W. Wang, T. Guo, S. Kou, W. Wang, L. Miao, X. Cao, J. Zhao, G. Yang, S. Zhang, H. Lian, H. Q. Yang, *Arabidopsis* cryptochrome 1 controls photomorphogenesis through regulation of H2A.Z deposition. *Plant Cell* **33**, 1961–1979 (2021).
37. H. Lian, P. Xu, S. He, J. Wu, J. Pan, W. Wang, F. Xu, S. Wang, J. Pan, J. Huang, H. Q. Yang, Photoexcited CRYPTOCHROME 1 interacts directly with G-protein β subunit AGB1 to regulate the DNA-binding activity of HY5 and photomorphogenesis in *Arabidopsis*. *Mol. Plant* **11**, 1248–1263 (2018).
38. C. Lin, H. Yang, H. Guo, T. Mockler, J. Chen, A. R. Cashmore, Enhancement of blue-light sensitivity of *Arabidopsis* seedlings by a blue light receptor cryptochrome 2. *Proc. Natl. Acad. Sci. U.S.A.* **95**, 2686–2690 (1998).
39. M. T. Osterlund, C. S. Hardtke, N. Wei, X. W. Deng, Targeted destabilization of HY5 during light-regulated development of *Arabidopsis*. *Nature* **405**, 462–466 (2000).
40. S. J. Clough, A. F. Bent, Floral dip: A simplified method for Agrobacterium-mediated transformation of *Arabidopsis* thaliana. *Plant J.* **16**, 735–743 (1998).
41. H. Guo, H. Yang, T. C. Mockler, C. Lin, Regulation of flowering time by *Arabidopsis* photoreceptors. *Science* **279**, 1360–1363 (1998).
42. B. Langmead, S. L. Salzberg, Fast gapped-read alignment with Bowtie 2. *Nat. Methods* **9**, 357–359 (2012).
43. G. Yu, L. G. Wang, Q. Y. He, ChIPseeker: An R/Bioconductor package for ChIP peak annotation, comparison and visualization. *Bioinformatics* **31**, 2382–2383 (2015).
44. F. Ramirez, F. Dundar, S. Diehl, B. A. Gruning, T. Manke, deepTools: A flexible platform for exploring deep-sequencing data. *Nucleic Acids Res.* **42**, W187–W191 (2014).
45. S. Lindoo, M. Caldwell, Ultraviolet-B radiation-induced inhibition of leaf expansion and promotion of anthocyanin production. *Plant Physiol.* **61**, 278–282 (1978).

Acknowledgments: We thank X. Chen (University of California, Riverside) for providing the *mac3a3b* double mutants, B. Yu (University of Nebraska-Lincoln) for providing the *pro35S::MAC3A^{Mut1}-GFP* and *pro35S::MAC3A^{Mut2}-GFP* lines, S. Yang (China Agricultural University) and H. Li (The Sainsbury Laboratory) for research discussions and manuscript reading, and the UCLA-FAFU Joint Research Center on Plant Proteomics and the UCLA-MCDB/BSCRC Microscopy Core for institutional support. **Funding:** This work was supported by the Young Taishan Scholars Program (to X.W.), the Shandong Provincial Natural Science Fund for Excellent Young Scientists Fund Program (overseas) 2023HWYQ-108 (to X.W.), NIH grant GM56265 (to C.L.), and the UCLA Sol Leshin Program (to C.L.). **Author contributions:** Conceived and designed the experiments: B.J., C.L., and X.W. Performed the experiments: B.J., T.Y., J.B., V.B., C.Z., T.Z., and J.S. Analyzed the data: B.J., J.S., and Z.Z. Wrote the paper: B.J. and X.W. Reviewed and edited the paper: C.L., B.J., and X.W. All authors read and approved the manuscript. **Competing interests:** The authors declare that they have no competing interests. **Data and materials availability:** All data needed to evaluate the conclusions in the paper are present in the paper and/or the Supplementary Materials. Sequencing data are available in the National Center for Biotechnology Information (NCBI) Gene Expression Omnibus (GEO) database (accession no. GSE220945).

Submitted 1 March 2023
Accepted 6 July 2023
Published 9 August 2023
10.1126/sciadv.adh4048

ScienceAdvances

Co-condensation with photoexcited cryptochromes facilitates MAC3A to positively control hypocotyl growth in *Arabidopsis*

Bochen Jiang, Zhenhui Zhong, Jun Su, Tengfei Zhu, Timothy Yueh, Jielena Bragasin, Victoria Bu, Charles Zhou, Chentao Lin, and Xu Wang

Sci. Adv., **9** (32), eadh4048.
DOI: 10.1126/sciadv.adh4048

Science Advances (ISSN) is published by the American Association for the Advancement of Science. 1200 New York Avenue NW, Washington, DC 20005. The title *Science Advances* is a registered trademark of AAAS.